NANOSYSTEMS:
PHYSICS, CHEMISTRY, MATHEMATICS

Abiev R.Sh., et al. *Nanosystems: Phys. Chem. Math.*, 2024, **15** (1), 115–121.
http://nanojournal.ifmo.ru
DOI 10.17586/2220-8054-2024-15-1-115-121

Original article

Synthesis of strontium fluoride nanoparticles in a microreactor with intensely swirling flows

Rufat Sh. Abiev[1,2], Andrey V. Zdravkov[1], Yuliya S. Kudryashova[1], Alexander A. Alexandrov[3], Sergey V. Kuznetsov[3], Pavel P. Fedorov[3]

[1]Institute of Silicate Chemistry I. V. Grebenshchikov RAS, St. Petersburg, Russia

[2]St. Petersburg State Institute of Technology, St. Petersburg, Russia

[3]Prokhorov General Physics Institute of the Russian Academy of Sciences, Moscow, Russia

Corresponding author: Pavel P. Fedorov, ppfedorov@yandex.ru

ABSTRACT The technique of micromixing was used for synthesis of SrF_2 nanopowders in a microreactor with intensely swirling flows. The chemical reaction between aqueous solutions of strontium nitrate ($C(Sr(NO_3)_2)$ = 0.15 – 0.45 M) and potassium fluoride (C(KF) = 0.3 – 0.9 M) was realized in a microreactor with intensely swirling flows with reagent consumption 1.5 – 3.5 L/min. Colloidal solutions were obtained, during the settling of which SrF_2 powders were isolated without crystallographic faceting. An increase in the rate of reagent flow has negligible effect on the size of coherent scattering regions D, while an increase in the concentration of solutions leads to an increase in D from $\sim$ 20 to $\sim$ 30 nm.

KEYWORDS strontium fluoride, precipitation, chemical reaction, micromixing

ACKNOWLEDGEMENTS This work was done as a part of State assignment of the Institute of Silicate Chemistry (Project No. 1021050501070-0-1.4.3 (0081-2022-0006)) and Prokhorov General Physics Institute RAS (Project No. 0097-2019-0017). The study was carried out using the equipment of the Collective Use Centers of Prokhorov General Physics Institute RAS and Kurnakov Institute of General and Inorganic Chemistry RAS.

FOR CITATION Abiev R.Sh., Zdravkov A.V., Kudryashova Yu.S., Alexandrov A.A., Kuznetsov S.V., Fedorov P.P. Synthesis of strontium fluoride nanoparticles in a microreactor with intensely swirling flows. *Nanosystems: Phys. Chem. Math.*, 2024, **15** (1), 115–121.

1. Introduction

Strontium fluoride SrF_2 is an ionic compound and dielectric with a large band gap. It crystallizes in a cubic *fcc* lattice, SSG *Fm*-3*m*. SrF_2 crystals, transparent in the UV, visible and IR ranges, are photonics materials [1]. Strontium fluoride occurs in nature as a rare mineral strontiofluorite [2]. Strontium fluoride easily dissolves fluorides of rare earth elements RF_3 to form solid solutions $Sr_{1-x}R_xF_{2+x}$ ($x \leq 0.5$) [3]. Single crystals and ceramics of strontium fluoride doped with the rare earth ions are used as laser elements [4–9], effective phosphors [10] and fluoride solid electrolytes [11]. At the same time, activated strontium fluoride powders are precursors of optical ceramics [12–19], single crystals [20, 21] and films, and are also of independent interest as phosphors [22–31], including as part of composites [32].

Various methods are used for the synthesis of strontium fluoride powders [33, 34], including precipitation from aqueous solutions [13–15, 35, 36], hydro- and solvothermal synthesis [37–51], synthesis from solutions in a melt (flux technique) [52–54], sol-gel [55–59], combustion synthesis [60, 61], synthesis using ionic liquids [52], thermal decomposition of precursors [62], high-energy ball milling [63], chemical reaction at the solution/vapor interface [64], etc. In the synthesis by precipitation from aqueous solutions by chemical reactions, various fluorinating agents were used – solutions of hydrofluoric acid [35], sodium fluoride [36, 65], potassium fluoride [13–15, 36, 65], and ammonium fluoride [12, 22, 36].

When synthesizing nanopowders, including nanofluorides, at the first exploratory stages of research, not enough attention is paid to the hardware design of the process. The main efforts are aimed at clarifying the functional characteristics of the samples obtained. However, when scaling processes, taking into account the need for reproducibility of product characteristics, the hardware factor comes to the fore.

The influence of the correctness of the conditions of mixing processes, especially micromixing, on the quality of synthesized materials still remains insufficiently evaluated in the processes of solution chemistry [66]. At the same time, the organization of such conditions that allow the reagents to be distributed at the molecular or ionic level with the necessary degree of uniformity of their distribution in micro-volumes is an obvious prerequisite for obtaining nanoparticles with specified characteristics. Previously, the possibility of synthesis of nanoscale particles of oxides and fluorides in microreactors with impinging jets [67–70] and in microreactors with intensely swirling flows [67, 71–74] was experimentally proved. The influence of specific energy dissipation rate on micromixing quality was demonstrated experimentally by means of iodide-iodate method widely used for microreactors with ultimate level of micromixing [74].

© Abiev R.Sh., Zdravkov A.V., Kudryashova Yu.S., Alexandrov A.A., Kuznetsov S.V., Fedorov P.P., 2024

The developed microreactor with impinging swirling flows of reagent solutions [67] allows one to realize a micromixing time of about 0.01 sec by creating a powerful swirling flow in a limited small volume (about 0.2 ml), where the main amount of energy is dissipated, and to carry out fine individual adjustment of the flow rate of solutions supplied to the reaction zone. The device is characterized by high performance.

This work is aimed to synthesis powders of strontium fluoride, pure and doped with erbium and ytterbium ions, by chemical precipitation reaction in a microreactor with swirling flows of reagent solutions.

2. Experimental details

2.1. Samples preparation

The design of the microreactor with impinging swirling flows is described in [72]. The reactor from pyrex glass has two tangentially arranged nozzles for the supply of the initial components and a nozzle for the discharge of products. Characteristic dimensions of the device: the diameter of the wide part of the body is 20 mm, the diameter of the narrow part (neck) is 4 mm, the diameters of the tangential pipes are 4 mm.

The solutions of the initial media are pumped from external tanks into the pipes with the specified flow rates Q. When the solutions of the initial media are fed into the tangential pipes, the flows are swirled. Moreover the circumferential and axial velocity vectors of the two mixed flows in the mixing chamber are directed in the opposite direction. In the neck zone, extremely intensive mixing of all the supplied components occurs, due, firstly, to the high level of velocities (axial and tangential) in this zone, and secondly, to the powerful shear field induced by high velocities.

The following reagents were used for the synthesis of strontium fluoride: strontium nitrate tetrahydrate $Sr(NO_3)_2 \cdot 4H_2O$ (pure grade), potassium fluoride dihydrate $KF{\cdot}2H_2O$ (pure grade), and distilled water. The synthesis was carried out at room temperature. The synthesis process can be described by the following equation:

$$Sr(NO_3)_2 \cdot 4H_2O + 2KF \cdot 2H_2O = SrF_2 \downarrow + 2KNO_3 + 6H_2O. \quad (1)$$

The obtained samples were taken within 1 – 2 minutes to minimize the growth of particles in the suspension and their aggregation. The sediment was washed by decantation (on the Buchner funnel, the sediment passed through the "green ribbon" filter with pores of 3 – 5 microns). Immediately after washing, the samples were dried in a drying box. We varied the flow rates Q (1.5, 2.5 and 3.2 l/min) and the concentrations of the initial solutions (0.15, 0.30, 0.45 M $Sr(NO_3)_2$). The concentration of potassium fluoride in the solution was twice as high to ensure stoichiometry. The prepared solutions were kept for at least 12 hours before the experiments.

2.2. Samples characterization

The synthesized powders were characterized by X-ray phase analysis (XRD) and scanning electron microscopy (SEM). XRD was performed on a Bruker Advanced D8 diffractometer (CuKα radiation). Lattice parameters (a) and coherent scattering regions (D) were calculated using the TOPAS software ($R_{wp} < 5$).

Morphology and particle size were carried out on a Carl Zeiss NVision 40 electron scanning microscope (Germany) with an Oxford Instruments X-MAX microprobe analyzer (UK) (80 mm^2) for the energy dispersive analysis (EDX).

3. Results and discussion

Synthesis conditions, lattice parameters, coherent scattering regions are summarized in Table 1. X-ray patterns are shown in Fig. 1, micrographs – in Fig. 2. According to X-ray diffraction data, well-formed strontium fluoride nanopowders were obtained in all cases. The product lattice parameters within the error range correspond to strontium fluoride ($a = 5.800$ Å, JCPDS card # 06-0262). The particles are spherical without agglomerations with mean size about 20 – 30 nm. The values of the coherent scattering regions D are weakly dependent on the flow rates (Fig. 3a), but they increase markedly with increasing concentrations of solutions (Fig. 3b).

Note that strontium fluoride nanoparticles obtained as a result of syntheses are not faceted. The absence of faceting at a low synthesis temperature is a sign of processes far from equilibrium, namely, a sign of a non-classical mechanism of crystal growth by agglomeration of nanoparticles [53].

4. Conclusion

The use of a reactor with intensively swirled flows in synthesis by the method of precipitation from aqueous solutions makes it possible to regulate the driving forces of the process under conditions of intensive mixing by changing the concentration of solutions and increasing the feed rate of reagents. The use of this technique makes it possible to scale the process and obtain kilogram quantities of powder in a continuous process. The possibility of using such a reactor is shown in the synthesis of strontium fluoride nanopowders by the reaction of strontium nitrate solutions with potassium fluoride. Powders with the size of coherent scattering regions of 18 – 32 nm were obtained.

The data obtained indicate that the change in the flow rates of reagents does not significantly affect the average size of the resulting particles. This result could be explained as follows: even at the lowest flow rate of supplied solutions within studied range (from 1.5 to 3.2 L/min) the specific energy dissipation rate in the microvolume of reagents contacting was

TABLE 1. Concentration of initial solutions C, flow rates Q, lattice parameter a, and values of coherent scattering regions D

No.	$C(Sr(NO_3)_2)$, M	C(KF), M	Q, L/min	Lattice parameter a, Å	D, nm
1	0.15	0.3	1.5	5.8003(1)	20.1(1)
2	0.30	0.6	1.5	5.8004(1)	25.8(1)
3	0.45	0.9	1.5	5.8008(1)	30.5(1)
4	0.15	0.3	2.5	5.7999(1)	20.4(1)
5	0.30	0.6	2.5	5.8006(1)	24.3(1)
6	0.45	0.9	2.5	5.8004(1)	32.4(1)
7	0.15	0.3	3.2	5.8008(1)	18.1(1)
8	0.30	0.6	3.2	5.8010(1)	22.0(1)
9	0.45	0.9	3.2	5.8010(1)	29.0(1)

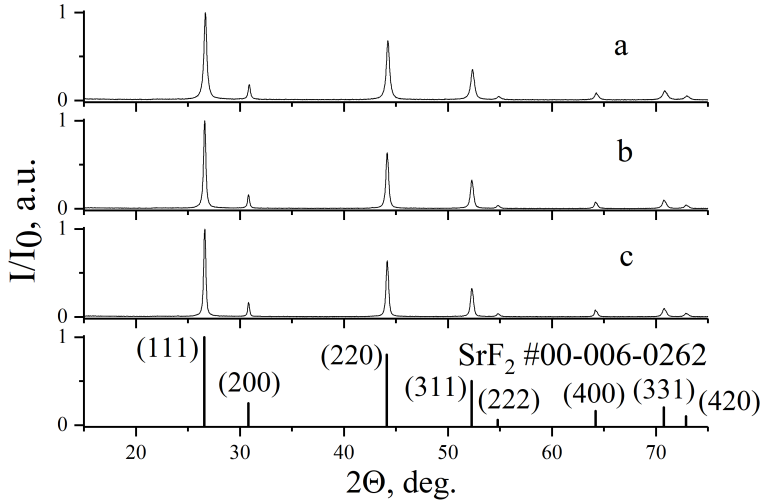

FIG. 1. XRD patters of the samples # 1(a), 2(b), 3 (c) and SrF_2

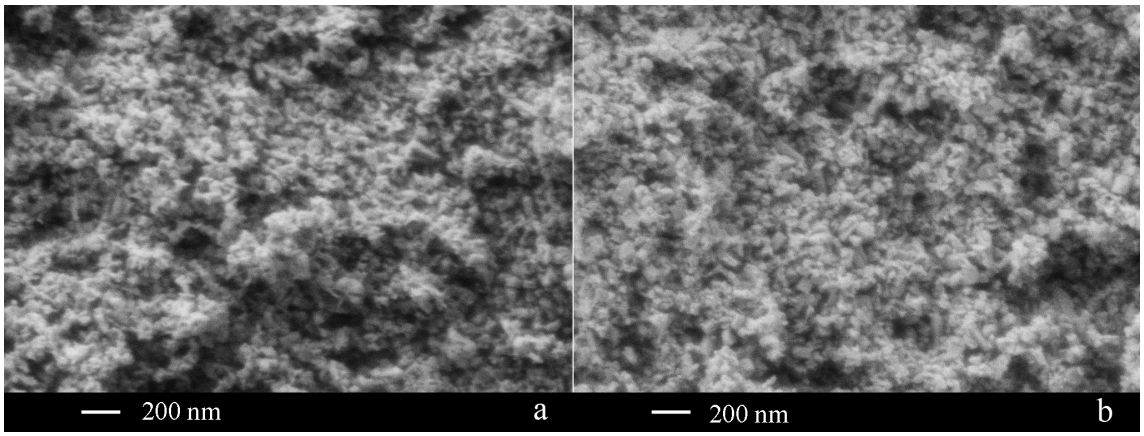

FIG. 2. SEM images of samples 1 (a) and 9 (b)

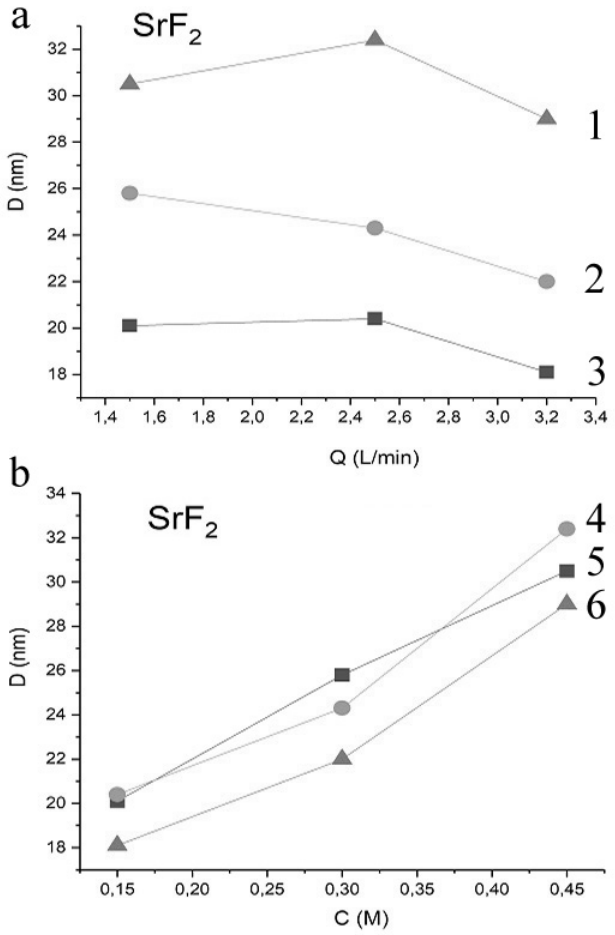

FIG. 3. The dependence of the coherent scattering values of D strontium fluoride nanoparticles synthesized in a reactor with swirling flows at different on the flow rates (a) and the concentration of strontium nitrate (b). Notations: M $Sr(NO_3)_2$ is equal to 0.45 (1); 0.30 (2); 0.15 (3); Q is equal to 2.5 L/min (4); 1.5 L/min (5); and 3.2 L/min (6).

high enough to ensure the necessary level of micromixing. This is consistent with the results obtained in the synthesis of calcium fluoride nanopowders using intensively swirled flows [67]. At the same time, as the concentration of reacting solutions increases, the particle size increases linearly in the first approximation.

Since the size of nanoparticles is an essential parameter regulating the luminescence intensity [74], the revealed patterns may be essential for optimizing technological processes, although the nature of them is not completely clear.

References

[1] Zverev V.A., Krivopustova E.V., Tochilina T.V. *Optical materials*. Part 2. St.-Petersburg: ITMO, 2013, 248 p. (in Russian)
[2] Yakovenchuk V.N., Ivanyuk G.Yu., Pakhomovsky Y.A., et al. Strontiofluorite, SrF_2, a new mineral species from the Khibiny massif, Kola peninsula, Russia. *The Canadian Mineralogist*, 2010, **48**, P. 1487–1492.
[3] Sobolev B.P., Seiranian K.B. *J. Solid State Chem.*, 1981, **39** (2), 17
[4] Kaminskii A.A. *Laser Crystals. Their Physics and Properties*. Berlin, Springer, 1990.
[5] Sobolev B.P. *The Rare Earth Trifluorides. Part 2. Introduction to materials science of multicomponent metal fluoride crystals*. Barcelona: Institut d'Estudis Catalans. 2001. 459 p.
[6] Moncorge R., Braud A., Camy P., Doualan J.L. Fluoride laser crystals. In: *Handbook on solid-state lasers: materials, systems and applications*. Ed. by B. Denker, E. Shklovsky. Oxford Cambridge Philadelphia New Delhi, Woodhead Publishing Limited, UK, 2013, p. 82–109.
[7] Druon F., Ricaud S., Papadopoulos D.N., Pellegrina A., Camy P., Doulan J.L., Moncorge R., Courjaud A., Mottay E., Georges P. On Yb:CaF_2 and Yb:SrF_2: review of spectroscopic and thermal properties and their impact on femtosecond and high power laser performance. *Opt. Mater. Express*, 2011, **1**, P. 489–502.
[8] Alimov O.K., Basiev T.T., Doroshenko M.E., Fedorov P.P., Konyuskin V.A., Nakladov A.N., Osiko V.V. Investigation of Nd^{3+} ions spectroscopic and laser properties in SrF_2 fluoride single crystal. *Opt. Mater.*, 2012, **34** (5), P. 799–802.
[9] Li W., Mei B., Song J. Nd^{3+}, Y^{3+}-codoped SrF_2 laser ceramics. *Opt. Mater.*, 2015, **47**, P. 108–111.

[10] Saleta Reig D., Grauel B., Konyushkin V.A., Nakladov A.N., Fedorov P.P., Busko D., Howard I.A., Richards B.S., Resch-Genger U., Kuznetsov S.V., Turshatov A., Würth C. Upconversion properties of SrF_2:Yb^{3+}, Er^{3+} single crystals. *J. Mat. Chem. C*, 2020, **8**, P. 4093–4101.

[11] Sorokin N.I., Sobolev B.P. Correlation between the Fluorine Ion Conductivities of $Sr_{1-x}R_xF_{2+x}$(CaF_2 Type) and $R_{1-y}Sr_yF_{3-y}$ (LaF_3 Type) Crystals in the SrF_2–RF_3 Systems (R = La–Nd). *Physics of the Solid State*, 2019, **61** (11), P. 2064–2069.

[12] Rozhnova Yu.A., Kuznetsov S.V., Luginina A.A., Voronov V.V., Ryabova A.V., Pominova D.V., Ermakov R.P., Usachev V.A., Kononenko N.E., Baranchikov A.E., Ivanov V.K., Fedorov P.P. New $Sr_{1-x-y}R_x(NH_4)_yF_{2+x-y}$ (R = Yb, Er) solid solution as precursor for high efficiency up-conversion luminophor and optical ceramics on the base of strontium fluoride. *Mater. Chem. Physics.*, 2016, **172**, P. 150–157.

[13] Zhu T., Mei B., Li W., Yang Y., Song J. Fabrication, microstructure and spectral properties of Nd:SrF_2 transparent ceramics with different concentration of La^{3+} ions. *Opt. Mater.*, 2019, **89**, P. 598–603.

[14] Gao Y., Mei B., Li W., Zhou Z., Liu Z. Effect of Yb^{3+} concentration on microstructure and optical properties of Yb: SrF_2 transparent ceramics. *Opt. Mater.*, 2020, **105**, 109869.

[15] Yi G., Mei B., Li W., Song J., Liu Z., Zhou Z., Su L. Synthesis and luminescence characterization of Pr^{3+}, Gd^{3+} co-doped SrF_2 transparent ceramics. *J. Am. Ceram. Soc.*, 2020, **103** (1), P. 279–286.

[16] Zheng C., Sun Z., Li W., Yang Y., Mei B. Fabrication and spectral properties of Dy: SrF_2 transparent ceramics. *Mater. Chem. Phys.*, 2021, **273**, 125141.

[17] Liu Z., Ji Y., Xu C., Wang Y., Liu Y., Shen Q., Yi G., Yu Y., Mei B., Liu P., Jing Qi. Microstructural, spectroscopic and mechanical properties of hot-pressed Er:SrF_2 transparent ceramics. *J. Eur. Ceram. Soc.*, 2021, **41**, P. 4907–4914.

[18] Yang Y., Zhou Z., Mei B., Zhang Y., Liu X. Fabrication and upconversion luminescence properties of Er:SrF_2 transparent ceramics compared with Er:CaF_2. *Ceram. Int.*, 2021, **47**, P. 17139–17146.

[19] Qin S., Song J., Wang W., Mei B., Li W., Xia Y. Study in optical and mechanical properties of Nd^{3+}, Y^{3+}: SrF_2 transparent ceramics prepared by hot-pressing and hot-forming techniques, *Crystals*, 2019, **619**.

[20] Arnold M., Katzmann J., Naik A., Görne A.L., Härtling T., George J., Schuster C. Investigations on electron beam irradiated rare-earth doped SrF_2 for application as low fading dosimeter material: evidence for and DFT simulation of a radiation-induced phase. *J. Mater. Chem. C*, 2022, **10**, P. 11579–11587.

[21] Yagoub Y.A., Swart H.C., Coetsee E. Luminescent behavior of SrF_2 and CaF_2 crystals doped with Eu ions under different annealing temperatures. *J. Alloys and Compd.*, 2021, **858**, 157741.

[22] Wolfbeis S. An overview of nanoparticles commonly used in fluorescent bioimaging. *Chem. Soc. Rev.*, 2015, **44**, P. 4743–4768.

[23] Richards B.S., Hudry D., Busko D., Turshatov A., Howard I.A. Photon upconversion for photovoltaics and photocatalysis. *Chem. Rev.*, 2021, **121**, P. 9165–9195.

[24] Brites C.D.S., Marin R., Suta M., Carneiro Neto A.N., Ximendes E., Jaque D., Carlos L.D. Spotlight on luminescence thermometry: basics, challenges, and cutting-edge applications. *Advanced Materials*, 2023, **35**, 2302749.

[25] Park C., Park S. Effective up-conversion behaviors for Er^{3+}–Yb^{3+}-doped SrF_2 phosphors synthesized by flux-assist method. *J. Mater. Sci. Mater. Electron.*, 2020, **31**, P. 832–837.

[26] Joseph R.E., Hudry D., Busko D., Biner D., Turshatov A., Krämer K., Richards B.S., Howard I.A. Bright constant color upconversion based on dual 980 and 1550 nm excitation of SrF_2:Yb^{3+}, Er^{3+} and β-$NaYF_4$:Yb^{3+}, Er^{3+} micropowders – considerations for persistence of vision displays. *Opt. Mater.*, 2021, **111**, 110598.

[27] Runowski M., Marciniak J., Grzyb T., Przybylska D., Shyichuk A., Barszcz B., Katrusiak A., Lis S. Lifetime nanomanometry – high-pressure luminescence of up-converting lanthanide nanocrystals – SrF_2:Yb^{3+},Er^{3+}. *Nanoscale*, 2017, **9**, P. 16030–16037.

[28] Ryszczynska S., Grzyb T. NIR-to-NIR and NIR-to-Vis up-conversion of SrF_2:Ho^{3+} nanoparticles under 1156 nm excitation. *Methods Appl. Fluoresc.*, 2022, **10**, 024001.

[29] Zeng Q., He W., Luan F., Yan Y., Du H., Fu J., Guo D. Insight into the mechanism of intense NIR-to-red upconversion luminescence in Er^{3+} doped and Er^{3+}–Yb^{3+} co-doped SrF_2 nanoparticles. *New J. Chem.*, 2021, **45**, P. 6469–6478.

[30] Yagoub M.Y.A., Swart H.C., Coetsee E. Structural, surface and luminescent properties of SrF_2:Eu annealed thin films. *Vacuum*, 2021, **191**, 110362.

[31] Yan Y., Tan Y., Li D., Luan F., Guo D. Efficient energy transfer, multi-colour emitting and temperature sensing behavior of single-phase Tb^{3+}, Eu^{3+} co-doped strontium fluoride phosphors. *J. Lumin.*, 2019, **211**, P. 209–217

[32] Luginina A.A., Kuznetsov S.V., Ivanov V.K., Voronov V.V., Yapryntsev A.D., Lyapin A.A., Chernova E.V., Pynenkov A.A., Nishchev K.N., Gaynutdinov R.V., Bogach A.V., Fedorov P.P. Laser damage threshold of hydrophobic up-conversion carboxylated nanocellulose/SrF_2:Ho composite films functionalized with 3-aminopropyltriethoxysilane. *Cellulose*, 2021, **28** (17), P. 10841–10862.

[33] Fedorov P.P., Luginina A.A., Kuznetsov S.V., Osiko V.V. Nanofluorides. *J. Fluorine Chem.*, 2011, **132** (12), P. 1012–1039.

[34] Karimov D.N., Demina P.A., Koshelev A.V.,. Rocheva V.V, Sokovikov A.V., Generalova A.N., Zubov V.P., Khaydukov E.V., Koval'chuk M.V., Panchenko V.Ya. Upconversion nanoparticles: synthesis, photoluminescence properties, and applications. *Nanotechnol. Russ.*, 2020, **15**, P. 655–678.

[35] Mayakova M.N., Luginina A.A., Kuznetsov S.V., Voronov V.V., Ermakov R.P., Baranchikov A.E., et al. Synthesis of SrF_2-YF_3 nanopowders by co-precipitation from aqueos solutions. *Mendeleev Communications*, 2014, **24** (6), P. 360–362.

[36] Ermakova Yu.A., Pominova D.V., Voronov V.V., Yapryntsev A.D., Ivanov V.K., Tabachkova N.Yu., Fedorov P.P., Kuznetsov S.V. Synthesis of SrF_2:Yb:Er ceramics precursor powder by co-precipitation from aqueous solution with different fluorinating media: NaF, KF, and NH_4F. *Dalton Trans.*, 2022, **51**, P. 5448–5456.

[37] Zhang C., Hou Z., Chai R., Cheng Z., Xu Z., Li C., Huang L., Lin J. Mesoporous SrF_2 and SrF_2:Ln^{3+} (Ln = Ce, Tb, Yb, Er) Hierarchical Microspheres: Hydrothermal Synthesis, Growing Mechanism, and Luminescent Properties. *J. Phys. Chem.*, 2010, **114**, P. 6928–6936.

[38] Chen D., Yu Y., Huang F., Huang P., Yang A., Wang Y. Modifying the Size and Shape of Monodisperse Bifunctional Alkaline-Earth Fluoride Nanocrystals through Lanthanide Doping. *J. Am. Chem. Soc.*, 2010, **132**, P. 9976–9978.

[39] Sun J., Xian J., Du H. Facile synthesis of well-dispersed SrF_2:Yb^{3+}/Er^{3+} upconversion nanocrystals in oleate complex systems. *Appl. Surf. Sci.*, 2011, **257**, P. 3592–3595.

[40] Sun J., Xian J., Zhang X., Du H. Hydrothermal synthesis of SrF_2:Yb^{3+}/Er^{3+} micro-/nanocrystals with multiform morphologies and upconversion properties. *J. Rare Earth*, 2011, **29**, P. 32–38.

[41] Peng J., Hou S., Liu X., Feng J., Yu X., Xing Y., Su Z. Hydrothermal synthesis and luminescence properties of hierarchical SrF_2 and SrF_2:Ln^{3+} (Ln = Er, Nd, Yb, Eu, Tb) micro/nanocomposite architectures. *Mater. Res. Bull.*, 2012, **47**, P. 328–332.

[42] Yagoub M.Y.A., Swart H.C., Noto L.L., O'Connel J.H., Lee M.E., Coetsee E. The effects of Eu-concentrations on the luminescent properties of SrF_2:Eu nanophosphor. *J. Lumin.*, 2014, **156**, P. 150–156.

[43] Yagoub M.Y.A., Swart H.C., Noto L.L., Bergman P., Coetsee E. Surface characterization and photoluminescence properties of Ce^{3+},Eu co-doped SrF_2 nanophosphor. *Materials*, 2015, **8**, P. 2361–2375.

[44] Quintanilla M., Cantarelli I.X., Pedroni M., Speghini A., Vetrone F. Intense ultraviolet upconversion in water dispersible SrF_2:Tm^{3+},Yb^{3+} nanoparticles: the effect of the environment on light emissions. *J. Mater. Chem. C*, 2015, **3**, P. 3108–3113.

[45] Li A.H., et al. Upconversion-luminescent/magnetic dual-functional sub-20 nm core-shell SrF_2:Yb,Tm@CaF_2:Gd heteronanoparticles. *Dalt. Trans.*, 2016, **45**, P. 5800–5807.

[46] Xie J., Bin J., Guan M., Liu H., Yang D., Xue J., et al. Hydrothermal synthesis and upconversion luminescent properties of Sr_2LaF_7 doped with Yb^{3+} and Er^{3+} nanophosphors. *J. Lumin.*, 2018, **200**, P. 133–140.

[47] Balabhadra S., Debasu M.L., Brites C.D.S., Ferreira R.A.S., Carlos L.D. Radiation-to-heat conversion efficiency in SrF_2:Yb^{3+}/Er^{3+} upconverting nanoparticles. *Opt. Mater.*, 2018, **83**, P. 1–6.

[48] Cortelletti P., Pedroni M., Boschi F., Pin S., Ghigna P., Canton P., et al. Luminescence of Eu^{3+} Activated CaF_2 and SrF_2 Nanoparticles: Effect of the Particle Size and Codoping with Alkaline Ions. *Cryst. Growth Des.*, 2018, **18** (2), P. 686–694.

[49] Przybylska D., Ekner-Grzyb A., Grześkowiak B.F., Grzyb T. Upconverting SrF_2 nanoparticles doped with Yb^{3+}/Ho^{3+}, Yb^{3+}/Er^{3+} and Yb^{3+}/Tm^{3+} ions – optimisation of synthesis method, structural, spectroscopic and cytotoxicity studies. *Scientific Reports*, 2019, **9**, 8669.

[50] Du S., Wang Y. A broad-range temperature sensor dependent on the magnetic and optical properties of SrF_2:Yb^{3+}/Ho^{3+}. *CrystEngComm.*, 2019, **21**, P. 1452–1457.

[51] Przybylska D., Grzyb T. Synthesis and up-conversion of core/shell SrF_2:Yb^{3+}/Er^{3+} @SrF_2:Yb^{3+},Nd^{3+} nanoparticles under 808, 975, and 1532 nm excitation wavelengths. *J. Alloys Compd.*, 2020, **831**, 154797.

[52] Fedorov P.P., Alexandrov A.A. Synthesis of inorganic fluorides in molten salt fluxes and ionic liquid mediums. *J. Fluorine Chem.*, 2019, **227**, 109374.

[53] Proydakova V.Yu., Alexandrov A.A., Voronov V.V., Fedorov P.P. Synthesis of Calcium and Strontium Fluorides Using Li_2SO_4–Na_2SO_4 Eutectic Melts. *Russ. J. Inorg. Chem.*, 2020, **65** (6), P. 834–838.

[54] Park C., Park S. Effective up-conversion behaviors for Er^{3+}–Yb^{3+}-doped SrF_2 phosphors synthesized by flux-assist method. *J. Mater. Sci.: Mater. Electron.*, 2020, **31** (1), P. 832–837.

[55] Ritter B., Haida P., Krahl T., Scholz G., Kemnitz E. Core-shell metal fluoride nanoparticles via fluorolytic sol-gel synthesis – a fast and efficient construction kit. *J. Mater. Chem. C*, 2017, **5** (22), P. 5444–5450.

[56] Ritter B., Haida P., Fink F., Krahl T., Gawlitza K., Rurack K., et al. Novel and easy access to highly luminescent Eu and Tb doped ultra-small CaF_2, SrF_2 and BaF_2 nanoparticles – structure and luminescence. *Dalton Transactions*, 2017, **46** (9), P. 2925–2936.

[57] Krahl T., Beer F., Relling A., Gawlitza K., Rurack K., Kemnitz E. Toward Luminescent Composites by Phase Transfer of SrF_2:Eu^{3+} Nanoparticles Capped with Hydrophobic Antenna Ligands. *ChemNanoMat.*, 2020, **6** (7), P. 1086–1095.

[58] Yusenko K.V., Kabelitz A., Schökel A., Wagner R., Prinz C., Kemnitz E., et al. Local Structure of Europium-Doped Luminescent Strontium Fluoride Nanoparticles: Comparative X-ray Absorption Spectroscopy and Diffraction Study. *ChemNanoMat.*, 2021, **7** (11), P. 1221–1229.

[59] Monks M.-J., Würth C., Kemnitz E., Resch-Genger U. Dopant ion concentration-dependent upconversion luminescence of cubic SrF_2:Yb^{3+}, Er^{3+} nanocrystals prepared by a fluorolytic sol-gel method. *Nanoscale*, 2022, **32**.

[60] Rakov N., Guimaraes R.B., Franceschini D.F., Maciel G.S. Er:SrF_2 luminescent powders prepared by combustion synthesis. *Mater. Chem. Phys.*, 2012, **135**, P. 317–321.

[61] Rakov N., Guimaraes R.B., Maciel G.S. Managing optical heating via Al^{3+}-doping in Er^{3+}:SrF_2 powder phosphors prepared by combustion synthesis. *DaltonTrans.*, 2019, **48** (14), P. 4589–4595.

[62] Glazunova T.Yu., Boltalin A.I., Fedorov P.P. Synthesis of calcium, strontium, and barium fluorides by thermal decomposition of trifluoroacetates. *Russ. J. Inorg. Chem.*, 2006, **51** (7), P. 983–987. https://doi.org/10.1134/S0036023606070011

[63] Heise M., Scholz G., Krahl T., Kemnitz E. Luminescent properties of Eu^{3+} doped CaF_2, SrF_2, BaF_2 and PbF_2 powders prepared by high-energy ball milling. *Solid State Sciences*, 2019, **91**, P. 113–118.

[64] Gulina L.B., Schäfer M., Privalov A.F., Tolstoy V.P., Murin I.V., Vogel M. Synthesis and NMR investigation of 2D nanocrystals of the LaF_3 doped by SrF_2. *J. Fluorine Chem.*, 2016, **188**, P. 185–190.

[65] Fedorov P.P., Mayakova M.N., Maslov V.A., Baranchikov A.E., Ivanov V.K., Pynenkov A.A., Uslamina M.A., Nishchev K.N. The solubility of sodium and potassium fluorides in the strontium fluoride. *Nanosystems: Physics, Chemistry, Mathematics*, 2017, **8** (6), P. 830–834.

[66] Falk L., Commenge J.-M. Performance comparison of micromixers. *Chem. Eng. Sci.*, 2010, **65**, P. 405–411.

[67] Abiev R.Sh., Zdravkov A.V., Kudryashova Yu.S., Alexandrov A.A., Kuznetsov S.V., Fedorov P.P. Syntheses of calcium fluoride nanoparticles in a microreactor with intensely swirling flows. *Russ. J. Inorg. Chem.*, 2021, **66** (7), P. 1049–1054.

[68] Abiev R.Sh. Impinging-Jets Micromixers and Microreactors: State of the Art and Prospects for Use in the Chemical Technology of Nanomaterials (Review). *Theor. Found. Chem.*, 2020, **54**, P. 1131–1147.

[69] Abiev R.Sh., Sirotkin A.A. Influence of Hydrodynamic Conditions on Micromixing in Microreactors with Free Impinging Jets. *Fluids*, 2020, **5** (4), 179.

[70] Proskurina O.V., Abiev R.Sh., Nevedomskiy V.N. Influence of using different types of microreactors on the formation of nanocrystalline $BiFeO_3$. *Nanosystems: Phys. Chem. Math.*, 2023, **14** (1), P. 120–126.

[71] Lomakin M.S., Proskurina O.V., Abiev R.Sh., Leonov A.A., Nevedomskiy V.N., Voznesenskiy S.S., Gusarov V.V. Pyrochlore phase in the Bi_2O_3–Fe_2O_3–WO_3–(H_2O) system: Physicochemical and hydrodynamic aspects of its production using a microreactor with intensively swirled flows. *Advanced Powder Technology*, 2023, **34**, 104053.

[72] Abiev R.S., Kudryashova Y.S., Zdravkov A.V., Fedorenko N.Y. Micromixing and Co-Precipitation in Continuous Microreactors with Swirled Flows and Microreactors with Impinging Swirled Flows. *Inorganics*, 2023, **11**, 49.

[73] Barashok K.I., Panchuk V.V., Semenov V.G., Almjasheva O.V., Abiev R.Sh. Formation of cobalt ferrite nanopowders in an impinging-jets microreactor. *Nanosystems: Phys., Chem., Math.*, 2021, **12** (3), P. 303–310.

[74] Pominova D., Romanishkin I., Proydakova V., Kuznetsov S., Grachev P., Ryabova A., Tabachkova N., Fedorov P., Loschenov V. Study of synthesis temperature effect on β-$NaGdF_4$: Yb^{3+}, Er^{3+} upconversion luminescence efficiency and decay time using maximum entropy method. *Methods and Applications in Fluorescence*, 2022, **10**, 024005.

Submitted 17 November 2023; revised 25 December 2023; accepted 26 December 2023

Information about the authors:

Rufat Sh. Abiev – Institute of Silicate Chemistry I. V. Grebenshchikov RAS, Makarova emb. 2, St. Petersburg, Russia 199034; St. Petersburg State Institute of Technology, Moskowsky Pr. 26, St. Petersburg, Russia 190013; ORCID 0000-0003-3571-5770; abiev.rufat@gmail.com

Andrey V. Zdravkov – Institute of Silicate Chemistry I. V. Grebenshchikov RAS, Makarova emb. 2, St. Petersburg, Russia 199034; ORCID 0000-0002-9056-0823; a.v.zdravkov@gmail.com

Yuliya S. Kudryashova – Institute of Silicate Chemistry I. V. Grebenshchikov RAS, Makarova emb. 2, St. Petersburg, Russia 199034; ORCID 0000-0003-2555-4969; kadulinajul@mail.ru

Alexander A. Alexandrov – Prokhorov General Physics Institute of the Russian Academy of Sciences, Vavilova str. 38, Moscow, Russia 119991; ORCID 0000-0001-7874-7284; alexandrov1996@yandex.ru

Sergey V. Kuznetsov – Prokhorov General Physics Institute of the Russian Academy of Sciences, Vavilova str. 38, Moscow, Russia 119991; ORCID 0000-0002-7669-1106; kouznetzovsv@gmail.com

Pavel P. Fedorov – Prokhorov General Physics Institute of the Russian Academy of Sciences, Vavilova str. 38, Moscow, Russia 119991; ORCID 0000-0002-2918-3926; ppfedorov@yandex.ru

Conflict of interest: the authors declare no conflict of interest.